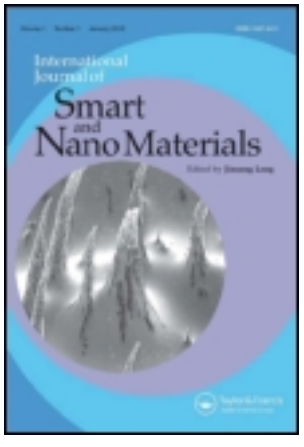

International Journal of Smart and Nano Materials

Publication details, including instructions for authors and subscription information:
http://www.tandfonline.com/loi/tsnm20

Melt-spun thin ribbons of shape memory TiNiCu alloy for micromechanical applications

A.V. Shelyakov [a], N.N. Sitnikov [a], V.V. Koledov [b], D.S. Kuchin [b], A.I. Irzhak [c] & N.Yu. Tabachkova [c]

[a] Department of Solid State Physics and Nanosystems, National Research Nuclear University "MEPhI", Kashirskoe shosse 31, 115409, Moscow, Russian Federation

[b] Department of Physics of Magnetic Phenomena, Kotelnikov Institute of Radio-Engineering and Electronics of Russian Academy of Sciences, Mohovaya st. 11/7, 125009, Moscow, Russian Federation

[c] Department of Material Science of Semiconductors and Dielectrics, National University of Science and Technology "MISiS", Leninsky prospect 4, 119049, Moscow, Russian Federation

Version of record first published: 30 Mar 2011.

To cite this article: A.V. Shelyakov , N.N. Sitnikov , V.V. Koledov , D.S. Kuchin , A.I. Irzhak & N.Yu. Tabachkova (2011): Melt-spun thin ribbons of shape memory TiNiCu alloy for micromechanical applications, International Journal of Smart and Nano Materials, 2:2, 68-77

To link to this article: http://dx.doi.org/10.1080/19475411.2011.567305

International Journal of Smart and Nano Materials
Vol. 2, No. 2, June 2011, 68–77

Melt-spun thin ribbons of shape memory TiNiCu alloy for micromechanical applications

A.V. Shelyakov[a]*, N.N. Sitnikov[a], V.V. Koledov[b], D.S. Kuchin[b], A.I. Irzhak[c] and N.Yu. Tabachkova[c]

[a]*Department of Solid State Physics and Nanosystems, National Research Nuclear University "MEPhI", Kashirskoe shosse 31, 115409 Moscow, Russian Federation;* [b]*Department of Physics of Magnetic Phenomena, Kotelnikov Institute of Radio-Engineering and Electronics of Russian Academy of Sciences, Mohovaya st. 11/7, 125009 Moscow, Russian Federation;* [c]*Department of Material Science of Semiconductors and Dielectrics, National University of Science and Technology "MISiS", Leninsky prospect 4, 119049 Moscow, Russian Federation*

(*Received 9 November 2010; final version received 25 February 2011*)

The development of micromechanical devices (MEMS and NEMS) on the basis of nanostructured shape memory alloys is reported. A $Ti_{50}Ni_{25}Cu_{25}$ (at. %) alloy fabricated by the melt spinning technique in the form of a ribbon with a thickness around 40 μm and a width about 1.5 mm was chosen as a starting material. Technological parameters were optimized to produce the alloy in an amorphous state. The thickness of the ribbon was reduced to 5–14 μm by means of electrochemical polishing. A nanostructural state of the thin ribbons was obtained via the dynamic crystallization of the amorphous alloy by application of a single electric pulse with duration in the range of 300–900 μs. A microtweezers prototype with a composite cantilever of 0.8 μm thick and 8 μm long was developed and produced on the basis of the obtained nanostructured thin ribbons by means of the focused ion beam technique. Controlled deformation of the micromanipulator was achieved by heating using semiconductor laser radiation in a vacuum chamber of scanning ion-probe microscope.

Keywords: melt-spun ribbon; shape memory alloy; composite micromanipulator; microtweezers

1. Introduction

Shape memory alloys (SMAs) are promising potential candidates for various novel technical applications. In recent years, they have impressively entered into such application fields as power, instrument and mechanical engineering, aerospace technology, and robotics. The new arising needs in the field of micro (nano)-electro-mechanical system (MEMS and NEMS) applications require small, cheap and fast responding devices based on such alloys [1–11]. This seriously motivates the necessity to develop new thin SMA materials. Recently melt-spinning and planar flow-casting techniques were used for production of SMA thin ribbons of a thickness in the range of 20–60 μm [12–17]. The rapidly quenched alloys of the quasi-binary TiNi–TiCu system with high Cu contents can feature an amorphous state at high cooling rates. Standard isothermal heat treatment

*Corresponding author. Email: avshelyakov@mephi.ru

ISSN 1947-5411 print/ISSN 1947-542X online

DOI: 10.1080/19475411.2011.567305
http://www.informaworld.com

of amorphous alloys results in formation of a microcrystalline structure and exhibition of a pronounced shape memory effect (SME). For micromechanical applications it is necessary to obtain thinner SMA ribbons (films) with ultrafine-grained structure. This paper presents an investigation of the influence of thinning the ribbon by electrochemical polishing and dynamic crystallization of the amorphous alloy on its microstructure and thermomechanical properties for the purpose of fabrication of a micromanipulator (microtweezers).

2. Experimental

The material under investigation was manufactured by a single-roller melt-spinning technique from a pre-synthesized $Ti_{50}Ni_{25}Cu_{25}$ (at. %) alloy. High purity nickel, titanium and copper were melted six times in an argon arc furnace. The obtained ingots were melted down in quartz crucibles under a purified atmosphere of inert gas and ejected onto the surface of a fast rotating copper wheel at cooling rates around 10^6 K/s. Thus, the rapidly quenched $Ti_{50}Ni_{25}Cu_{25}$ alloy was prepared in the form of continuous (10–30 m long) ribbon with a thickness in the range 30–50 μm and a width about 1.5 mm.

Alloy ribbon samples were thinned by electrochemical polishing, using electrolyte PLS-3® on the base of thiourea and sulfuric acid with complexing agents produced by TECHNOCOM AS company (http://www.technocom-as.ru). The applied voltage and current density were 5 V and 30–50 mA/cm^2, respectively, at an operation temperature of 20°C.

Thinned ribbon samples were crystallized by a special method of dynamic crystallization of the amorphous alloy. The experimental facility allowed one to heat an amorphous sample by controlled single pulse of electrical current with a given duration and amplitude. To provide the heat energy required for heating up the sample up to crystallization temperature, the relationship between the current density value J and the duration Δt of the electric pulse was calculated from

$$J(\Delta t) = \frac{1}{\sqrt{\Delta t}}\sqrt{C \cdot \Delta T \frac{\rho_V}{\rho}}\ , \tag{1}$$

where ρ_V is the density of the amorphous ribbon, ρ the electrical resistivity of the amorphous ribbon, C the specific heat capacity of the amorphous ribbon, and ΔT the temperature interval from ambient temperature to that of crystallization.

The surface structure of the samples was observed by scanning electron microscope (SEM, FEI Quanta 600 FEG®). The microstructure observations were performed using a JEM 2100 transmission electron microscope.

The shape memory behavior of the studied melt-spun TiNiCu alloys was characterized by strain–temperature curves obtained by thermal cycling of the ribbon samples through the transformation range under constant stress.

Samples of micromechanical device were prepared out of the $Ti_{50}Ni_{25}Cu_{25}$ alloy ribbon by the focused ion beam (FIB) technique on a Strata FIB 201® setup (FEI company).

3. Results and discussion

3.1. Thinning melt-spun ribbon by electrochemical polishing

The melt-spinning process for the studied alloy is known to produce mainly the amorphous state of the ribbons after solidification [14,16]. A typical cross-section of the ribbons is presented in Figure 1 and characterized by slightly variable thickness.

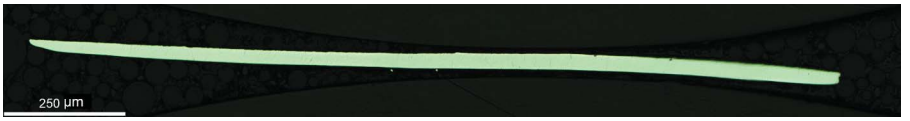

Figure 1. Optical micrograph of a typical cross-section of melt-spun ribbons.

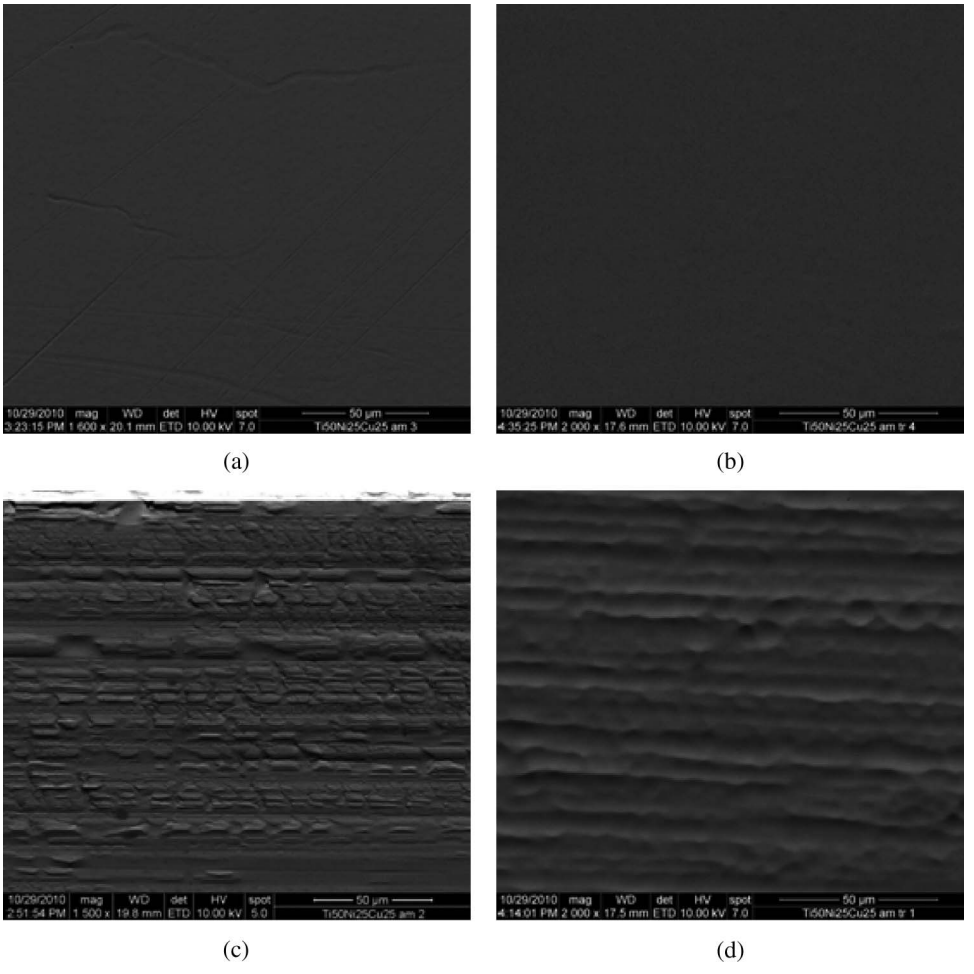

Figure 2. SEM micrographs of the 'free' (a, b) and 'contact' (c, d) surface of the $Ti_{50}Ni_{25}Cu_{25}$ (at. %) melt-spun ribbons: (a, c) untreated (initial melt-spun); (b, d) thinned (after electrochemical polishing).

Fabricated amorphous ribbons were thinned by electrochemical polishing. The advantage of electropolishing is that the thinning rate can be controlled by the applied voltage. Under the conditions 5 V, 30–50 mA/cm^2 at 20°C, the polishing rate was about 0.5–0.6 µm/min. The amorphous $Ti_{50}Ni_{25}Cu_{25}$ alloy ribbon with initial thickness 37 µm was polished in 50 minutes providing thin ribbons with thickness around 12 µm and 40 mm long. Typical SEM micrographs of the 'free' and 'contact' surfaces of untreated (initial melt-spun) and thinned (after electrochemical polishing) ribbons are shown in Figure 2. It can be seen that in the process of electrochemical machining both the thinning and the

polishing of the samples occur, in particular some irregularities disappear and the surface becomes smoother. It should be noted that this technique allows obtaining continuous-solid samples of amorphous ribbons with thickness down to 5 μm.

3.2. Microstructure of dynamically crystallized ribbons

Dynamic annealing of the thinned ribbons was performed in air without any protection. Following calculations from the forgoing equation, the pulse amplitude and duration (Figure 3) were chosen to provide heat energy release required for the sample crystallization. A number of the samples with time of crystallization in the range 300–900 μs were prepared.

After electrochemical polishing the ribbon structure remained amorphous as revealed by TEM investigations (Figure 4a). Dynamic crystallization of the thinned ribbons with necessary current density for various times of crystallization resulted in the formation of colonies of fine 60–80 nm thick martensite plates. The corresponding characteristic TEM images for the thinned samples with time of crystallization 600 μs are presented in Figure 4b and Figure 4c. In case of insufficient current density, a partially crystallized state was observed (Figure 4d).

3.3. Thermomechanical property measurements

The shape memory behavior of the ribbons was studied by an experimental setup for which a schematic representation is shown in Figure 5. The setup included a bending press with overall dimensions of 10×5×6 mm made of brass and consisted of two parts with several raised portions (teeth). The studied sample was placed between these indented parts. The upper part of the press was provided by a load and connected with a wire frame. The shift of the frame was controlled by a differential optical sensor consisted of infrared LED and back-to-back photodiodes. A heater in the lower part of the press allowed one to vary the sample temperature that was controlled by thermocouple. The LED radiation was modulated by audio-frequency for noise reduction. The measurements were controlled by a computer with analog-to-digital and digital-to-analog card.

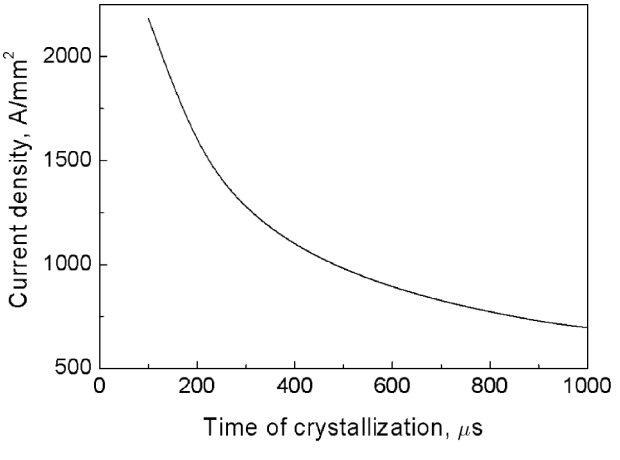

Figure 3. Current density vs. the time of dynamic crystallization.

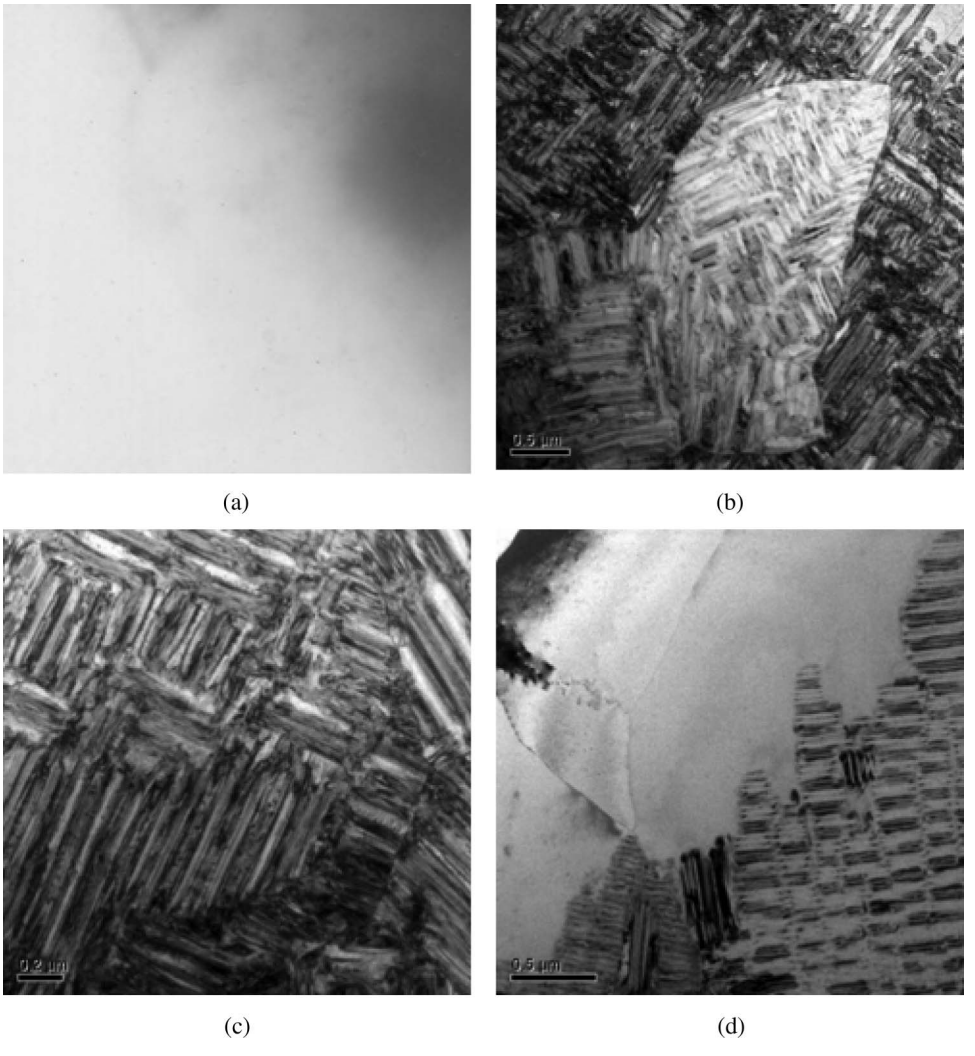

Figure 4. TEM micrographs of the thinned rapidly quenched $Ti_{50}Ni_{25}Cu_{25}$ (at. %) alloy at an initial state (a) and after dynamic crystallization at 600 μs: (b, c) completely crystallized state; (d) partially crystallized state.

In initial condition at ambient temperature the sample was deformed under the applied load. On heating the sample material started undergoing reverse martensitic transformation, and as a result the sample begun to recover the unstrained shape and lifted the upper part of the press. The shift of the upper part was fixed by the sensor and displayed on the computer screen. On cooling the sample returned in initial deformed state. The control program allowed one to thermocycle the sample through the transformation range under different constant stresses.

The characteristic dependence of the bending strain on temperature is shown in Figure 6 for the samples of 12 μm thick that were dynamically crystallized in 600 μs and for comparison isothermally annealed in a furnace at 500°C in 180 s. It was established from the obtained strain–temperature curves that the shape memory behavior was

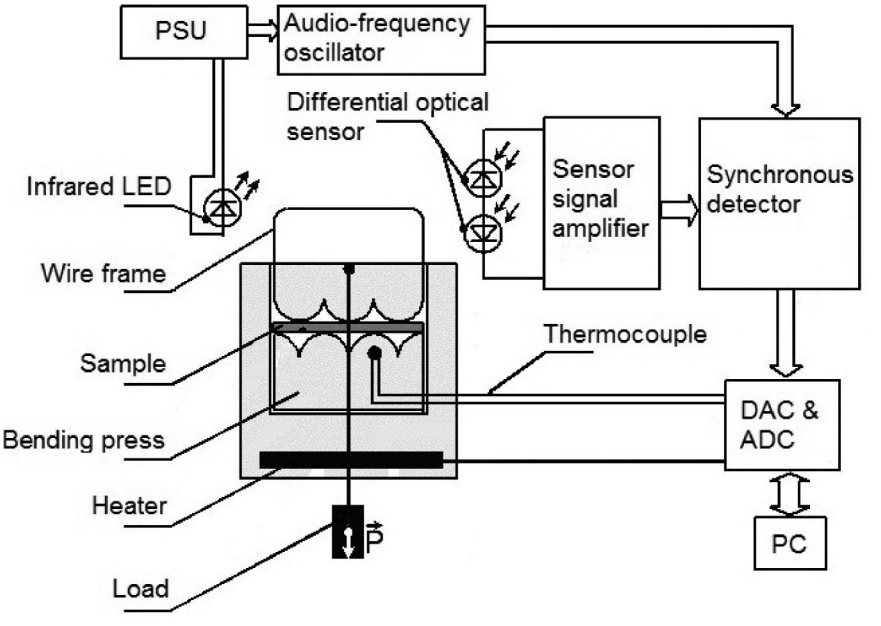

Figure 5. Schematic representation of experimental setup for thermomechanical measurements of SME alloys.

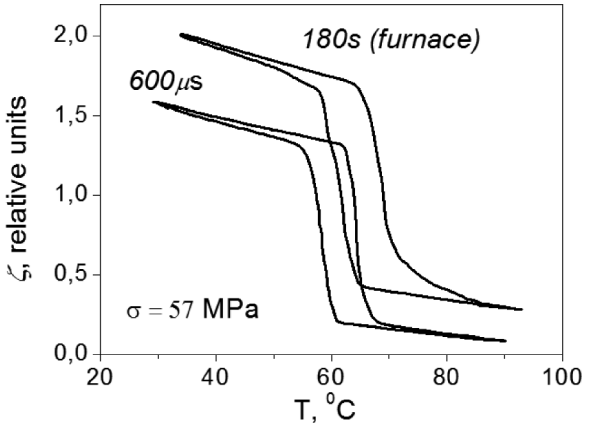

Figure 6. Typical strain vs. temperature curves under constant stress of the $Ti_{50}Ni_{25}Cu_{25}$ melt-spun ribbons.

very similar for both regimes of crystallization but dynamically crystallized ultrafine-grained samples had lower shape recovery temperatures. The maximum value of measured completely recovered bending strain was 7%.

3.4. Fabrication of composite micromanipulator (microtweezers)

Nanostructured thin ribbons of the melt-spun $Ti_{50}Ni_{25}Cu_{25}$ alloy were further used to develop and fabricate micromechanical devices. Recently, composite materials with

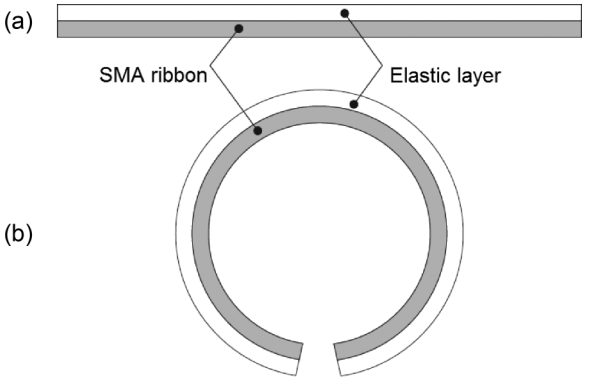

Figure 7. Principle of operation of the composite actuator based on a SMA ribbon: (a) on cooling and (b) on heating.

reversible SME that do not need training in order to obtain multiple reversible deformations have attracted much interest. The proposed composite material consists of a SMA ribbon (film) and an elastic layer of usual metal, which are tightly connected with each other (Figure 7). Prior to the connection, the SMA ribbon was given a pseudoplastic tensile deformation. The process of connecting the layers was carried out at a temperature below that of the reverse martensite transformation. As a result, the composite acquired the ability to perform a significant reversible bending deformation. This ability is based on the fact that the bending deformation of a composite plate consists of contraction on the inner side and extension on the outer side. On heating, the SMA layer exhibits contraction, thus producing tensile deformation in the elastic layer and bending in the composite (Figure 7b). On cooling, the SMA layer returns to the martensite state, whereby the elastic layer contracts and compresses the SMA layer, thus restoring the initial straightened shape (Figure 7a). The detailed description of this composite scheme can be found in [18].

On the basis of the proposed scheme, a microtweezers prototype has been developed and fabricated. The procedure of preparing the micromanipulator was the following (Figure 8). The thinned SMA ribbon was subjected to pseudoplastic tensile prestrain of 3% in the martensite state. A flat surface was formed on the edge that is codirectional with the pseudoplastic strain. Then an elastic platinum layer of the thickness around 400 nm was applied on the flat edge by ion-induced chemical vapor deposition (CVD) in the FIB setup, as shown in Figure 8a. Using the FIB technique a microtweezers prototype was formed in the ribbon with a gap at the end, which provided the possibility of controlled reversible bending (Figure 8b). Figures 8c and 8d present a scheme and a general view of the microtweezers prototype with a composite cantilever of 0.8 μm thick and 8 μm long.

Finally, the microtweezers were mounted to the end of the tip of micromanipulator Omniprobe 100, as shown in Figure 9a. Heating the SMA layer above the temperature of reverse martensitic transformation induced its contraction (compression) and as a result bending deformation of the cantilever. Cooling the bent composite below the martensitic transition temperature, the elastic layer, returning to the relaxed state, again pseudoplastically deformed the SMA layer and straightened the composite. Thus the micromanipulator (microtweezers) exhibited reversible deformation such that the opening varied from 1200 to 0 nm under the influence of an external source of thermal energy, for example, radiation of a semiconductor laser diode based on a GaAl/GaAlAs heterostructure.

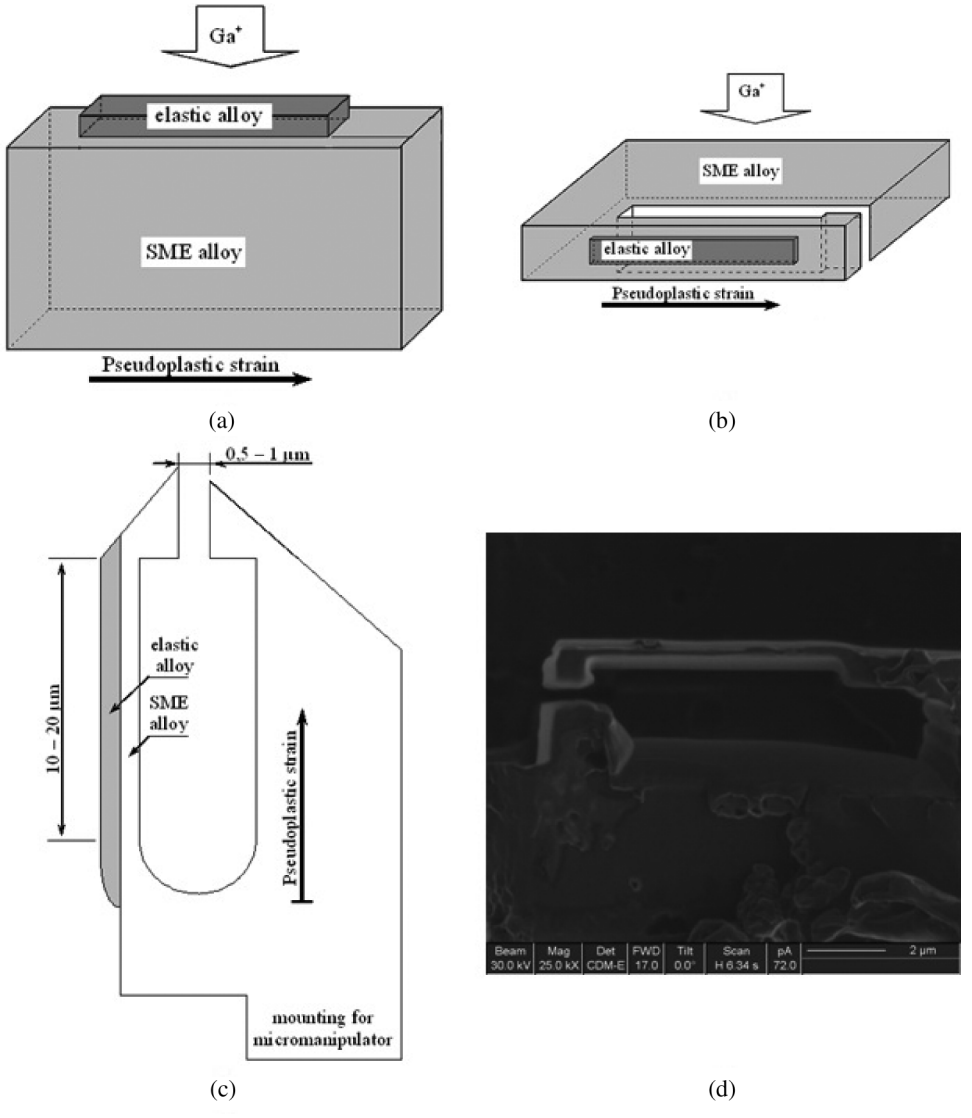

Figure 8. Scheme of preparation (a, b, c) and general view (d) of the microtweezers prototype on the base of the nanostructured thin ribbons of melt-spun shape memory $Ti_{50}Ni_{25}Cu_{25}$ alloy.

Figure 9 presents a three-dimensional manipulation of graphene sheets (located on a surface of a crystal of pyrolitic graphite) by means of the microtweezers prototype on a needle of micromanipulator Omniprobe. A video with CNT 3D manipulation is availably in the Internet on reference address: http://www.youtube.com/watch?v=pEGL_IcLxDs.

4. Concluding remarks

Thin amorphous TiNiCu ribbons of thickness 5–14 μm were produced by the melt-spinning technique with subsequent electrochemical polishing.

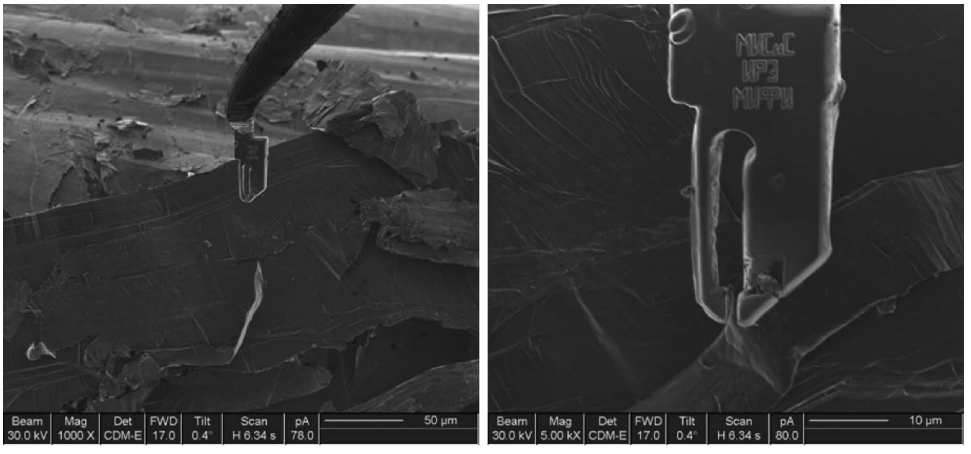

(a) (b)

Figure 9. 3D manipulation of graphene sheets by means of the microtweezers prototype on a needle of micromanipulator Omniprobe.

TEM investigations have shown that the dynamic crystallization of the amorphous $Ti_{50}Ni_{25}Cu_{25}$ alloy via single electric pulse application with a duration in the range 300–900 μs results in a considerable refinement of the alloy structure. This is accompanied by development of nanosized martensitic plates (20–60 nm).

Thermomechanical measurements have confirmed that dynamically crystallized ultrafine-grained ribbons exhibit a pronounced shape memory effect with completely recovered bending strain up to 7%.

The possibility of fabricating a composite micromanipulator (microtweezers) on the basis of the obtained nanostructured thin ribbons of the melt-spun shape memory $Ti_{50}Ni_{25}Cu_{25}$ alloy has been demonstrated by means of the FIB technology. A full nanotechnological procedure (selection of nanoobject – removal by microtweezers – replacement – release of the microtweezers) was realized for the example of graphene sheets.

Acknowledgments

This work has been carried out in the frames of Federal Target Program of Russian Federation, GK No. P726 and No. 14.740.11.0687.

References

[1] R.X. Wang, Y. Zohar, and M. Wong, *Residual stress-loaded titanium–nickel shape-memory alloy thin-film micro-actuators*, J. Micromech. Microeng. 12 (2002), pp. 323–327.
[2] J. Lee and S. Kim, *Manufacture of a nanotweezer using a length controlled CNT arm*, Sensor Actuator Phys. 120 (2005), pp. 193–198.
[3] H. Fujita, H. Toshiyoshi, G. Hashiguchi, and Y. Wada, *Micromachined tools for nanotechnology*, Riken Rev. 36 (2001), pp. 12–15.
[4] C. Clevy, A. Hubert, J. Agnus and N. Chaillet, *A micromanipulation cell including a tool changer*, J. Micromech. Microeng. 15 (2005), pp. S292– S301.
[5] Y.Q. Fu, J.K. Luo, A.J. Flewitt, S.E. Ong, S. Zhang, H.J. Du, and W.I. Milne, *Microactuators of free-standing TiNiCu films*, Smart Mater. Struct. 16 (2007), pp. 2651–2657.

[6] Y.Q. Fu, J.K. Luo, S.E. Ong, S. Zhang, A.J. Flewitt, and W.I. Milne, *A shape memory microcage of TiNi/DLC films for biological applications*, J. Micromech. Microeng. 18 (2008), 035026.
[7] K. Kim, X. Liu, Y. Zhang, and Y. Sun, *Nanonewton force-controlled manipulation of biological cells using a monolithic MEMS microgripper with two-axis force feedback*, J. Micromech. Microeng. 18 (2008), 055013.
[8] J.K. Luo, A.J. Flewitt, S.M. Spearing, N.A. Fleck, and W.I. Milne, *Comparison of microtweezers based on three lateral thermal actuator configurations*, J. Microelectromech. Syst. 15 (2005), pp. 1294–1302.
[9] J. Singh, T. Gan, A. Agarwal, and S. Liw, *3D free space thermally actuated micromirror device*, Sensor Actuator 123–124 (2005), pp. 468–475.
[10] M. Tomozawa, H. Kim, and S. Miyazaki, *Microactuators using R-phase transformation of sputter-deposited Ti–47.3Ni shape memory alloy thin films*, J. Intell. Mater. Syst. Struct. 17 (2006), pp. 1049–1058.
[11] L. Wu and H. Xiea, *A large vertical displacement electrothermal bimorph microactuator with very small lateral shift*, Thin Solid Film 447–448 (2004), pp. 148–152.
[12] R. Santamarta, E. Cesari, J. Pons, and T. Goryczka, *Shape memory properties of Ni–Ti based melt-spun ribbons*, Metall. Mater. Trans. A 35 (2004), pp. 761–766.
[13] S.H. Chang, S.K. Wu, and H. Kimura, *Shape memory effect of $Ti_{50}Ni_{25}Cu_{25}$ melt-spun ribbons crystallized under isothermal annealing*, Intermetallics 15 (2007), pp. 233–247.
[14] N.M. Matveeva, V.G. Pushin, A.V. Shelyakov, Yu.A. Bykovsky, S.B. Volkova, and V.S. Kraposhin, *Effect of conditions of crystallization of amorphous TiNi-TiCu alloys on structure and shape memory*, Phys. Met. Metalloved 83 (1997), pp. 626–632.
[15] H. Rösner, A.V. Shelyakov, A.M. Glezer, and P. Schlossmacher, *On the origin of the two-stage behavior of the martensitic transformation of $Ti_{50}Ni_{25}Cu_{25}$ melt-spun ribbons*, Mater. Sci. Eng. A 307 (2001), pp. 188–189.
[16] P. Schlossmacher, N. Boucharat, G. Wilde, H. Roesner, and A.V. Shelyakov, *Crystallization studies of amorphous melt-spun $Ti_{50}Ni_{25}Cu_{25}$*, J. Phys. IV 112 (2003), pp. 731–734.
[17] N. Resnina, S. Belyaev, and A. Shelyakov, *Martensitic transformation in amorphous-crystalline Ti–Ni–Cu and Ti–Hf–Ni–Cu thin ribbons*, Eur. Phys. J. Spec. Top. 158 (2008), pp. 21–26.
[18] A.V. Irzhak, V.S. Kalashnikov, V.V. Koledov, D.S. Kuchin, G.A. Lebedev, P.V. Lega, N.A. Pikhtin, I.S. Tarasov, V.G. Shavrov, and A.V. Shelyakov, *Giant reversible deformations in a shape memory composite material*, Tech. Phys. Lett. 36 (2010), pp. 329–332.